

## Investigation of Half-Metallic, Magnetic, and Thermodynamic Properties of Quaternary Half-Heusler NiCoFeX(X=S,As and Ge) using First-Principle Calculations

<sup>1</sup>Ogundola Sunday and <sup>2</sup>Temenu Funmilayo M.

<sup>1</sup>Department of Physics, University of Benin, Edo state, Nigeria.

<sup>2</sup>Department of Applied Geophysics, Federal University of Technology Akure, Ondo state, Nigeria.

\*Corresponding author: Email: [ogundolasunday01@gmail.com](mailto:ogundolasunday01@gmail.com) Phone: +2348032821353

### ABSTRACT

The First Principle Density Functional Theory (DFT) method was used to investigate the half-metallic character, magnetic and thermodynamic properties of NiCoFeX(X=Si,As and Ge). Electronic and magnetic properties such as band structures, densities of states, and magnetic moments, spin – polarization indices of each alloy are also determined to confirm half-metallicity and ferromagnetism. Thermodynamic properties such as Free Energy, Entropy, Heat Capacity and Debye Temperature are also computed using Quantum Espresso-based Thermo\_pw code. The half-metallic band gaps of NiCoFeAs, NiCoFeSi and NiCoFeGe are 0.206eV, 0.205eV and 0.203eV respectively. The spin-up channels in the electronic band structures of NiCoFeX(X=Si,As and Ge) have indirect energy band gap, indicating that they exhibit half-metallic character. The quaternary Heuslers NiCoFeX(X=Si,As and Ge) are accurately ferromagnetic as they all obey Slater Paulin's rule having magnetic moments of 4.0215 $\mu$ B, 4.1573 $\mu$ B and 4.6711 $\mu$ B respectively and are 100% spin-polarized. The Curie Temperatures  $T_c$  of NiCoFeX(X=Si,As and Ge) are 827K, 3631K and 827K respectively ( above the room temperature of 300K). However, only NiCoFeAs, and NiCoFeGe preserved their ferromagnetism after undergoing strain field. This makes them preferable candidates in the field of semiconductor physics. The heat capacities of NiCoFeX(X=Si,As and Ge) obey Dulong-petit law showing that they have good thermal applications in optoelectronic devices e.g. magnetic tunnel Junctions (MTJs), giant magneto-resistance devices (GMRs), Photo diodes, Solar cells etc.

### Keywords:

Heuslers,  
Density functional Theory,  
Half-metallicity.

### INTRODUCTION

Heusler compounds or alloys are magnetic intermetallics with face-centered cubic crystal structure and a composition of XYZ, where X and Y are transition metals and Z is in the p-block. There are five types of Heusler alloys or compounds, viz; XYZ is half-Heusler,  $X_2YZ$  is full-Heusler,  $XX^1YZ$  is quaternary Heusler,  $X_2Z$  is binary half-Heusler and  $X_3Z$  is binary full-Heusler. A Heusler can be semiconductor, metal or half-metal, but it is not an insulator. (Akriche *et al.*,2017) Every Heusler has spin-up and spin-down channels in its electronic band structure. If both spin-up and spin-down channels are metals, the half-Heusler is a metal. If one spin is semiconductor and the other is a metal, then it is half-metallic or a half-metal (Atifi *et al.*,2016). Lastly, if both spins are semiconductors then the heusler is a semiconductor. Many of these compounds exhibit

properties relevant to spintronics such as magnetoresistance, variations of the Hall effect, ferro, antiferro, and ferrimagnetism, half-metallicity, semiconductivity with spin filter ability, superconductivity, and topological band structure. Their magnetism results from a double-exchange mechanism between neighbouring magnetic ions in the first Heusler compound discovered. Heuslers derived its name after a German Engineer and Chemist Friedrich Heusler, who studied such a compound,  $Cu_2MnAl$  in 1903 which contained copper, manganese and Aluminum. Heuslers are isoelectronic compounds that are promising thermoelectric materials because of their high power factor and thermal stability. The magnetic materials particularly of the crystallographic phase  $Cl_b$  of the half-Heusler compounds have been an active field of research, as a consequence of their frequently emerging novel

properties and field of application since their first discovery by Friedrich Heusler in 1903 with the composition of  $\text{Cu}_2\text{MnAl}$  which behaves like a ferromagnet (Babiker *et al.*,2017). In 1983, De Groot *et al* discovered half-metallic ferromagnetism in half-Heusler and further revealed their potentials for promising technological applications (Atifi *et al.*,2016).Also, the importance of these materials has been uncovered by viewing the novel features of the electronic band structure and magnetic behaviour of quaternary Heuslers  $\text{NiCoFeX}$  ( $\text{X}=\text{Si,As}$  and  $\text{Ge}$ ). Over 400 of the Heusler alloys are predicted to be useful as topological insulators and thermoelectric materials (Bloch *et al.*,2018). In the same vein, over 350 heuslers are recognized to have good applications in optoelectronics, magnetic tunnel junctions, giant magneto-resistant devices, piezoelectric semiconductors etc. Extensive investigation is carried out on the possibility of half-metallicity and ferromagnetism of the quaternary heuslers  $\text{NiCoFeX}(\text{X}=\text{Si,As}$  and  $\text{Ge}$ ) using Density functional theory approach (Born *et al.*,2016). The target of recent research related to Heusler materials is to investigate ferromagnetic quaternary heusler compounds exhibiting the magnetic field induced super-elasticity, and large strain-induced changes in the magnetization. Over 400 of the Heusler alloys are predicted to be useful as topological insulators and thermometric materials (Bahnes *et al.*,2016). Also, over 350 quaternary Heusler alloys are recognized to have good applications in spintronic, optoelectronics, magnetic tunnel functions, giant magneto-resistant devices and piezoelectric semiconductors (Chibani *et al.*,2018). Extensive investigation is carried out on the possibility of half-metallicity and ferromagnetism of the quaternary Heuslers  $\text{NiCoFeX}(\text{X}=\text{Si,As}$  and  $\text{Ge}$ ) using first principle calculations.

## MATERIALS AND METHODS

Using quantum espresso that implements Density Functional Theory (DFT), properties of quaternary Heuslers  $\text{NiCoFeX}(\text{X}=\text{Si,As}$  and  $\text{Ge}$ ) are calculated.

Extension of electron wave function is done by the plane wave basis set (Fazian *et al.*,2016).The Perdew-Burke-Ernzerhot (PBE) type of generalized gradient approximation (GGA) of the exchange correlation functional is selected for accuracy of eigen energy obtained.The ultrasoft version of pseudopotential is selected (Babalola and Iyorzor,2019). Variable cell relaxation is carried out together with the geometric optimization to compute the structural properties of  $\text{NiCoFeX}(\text{X}=\text{Si,As}$  and  $\text{Ge}$ ). Plane wave basis set of kinetic energy cut-off of 1256eV and 1082eV are used, and Monkhorst pack mesh of  $10 \times 10 \times 10$ ,  $9 \times 9 \times 9$  and  $8 \times 8 \times 8$  in the brilloun zone of  $\text{NiCoFeX}(\text{X}=\text{Si,As}$  and  $\text{Ge}$ ) are respectively used (Feng *et al.*,2015). The magnetic moments, spin-polarized band structures and their densities of states (dos) are also computed. The mechanical and thermodynamic properties of  $\text{NiCoFeX}(\text{X}=\text{Si,As}$  and  $\text{Ge}$ ) are calculated using quantum espresso –based thermos\_pw code.

## RESULTS AND DISCUSSION

### Total Energy and Structural Properties

Total energy as a function of lattice constants for the ferromagnetic (FM) and non-magnetic (NM) of  $\text{NiCoFeX}(\text{X}=\text{Si, As and Ge})$  is computed as shown in Fig. 3.1. It is observed that the ferromagnetic status of  $\text{NiCoFeGe}$  is optimized at lowest energy, followed by the ferromagnetic status of  $\text{NiCoFeAs}$  and  $\text{NiCoFeSi}$  which are almost optimized at the same energy.This indicates that  $\text{NiCoFeGe}$  is more ferromagnetic than the others (Bainsla *et al.*,2016). This is as a result of germanium being a semiconductor while arsenic and silicon are non-metals, although the presence of Ni, Co and Fe as ferromagnetic elements contribute immensely to the ferromagnetic character of the quaternary heusler alloys. Total energy as a function lattice constants ( $\text{\AA}$ ) in the ferromagnetic states is fitted to the Birch-Murnaghan equation of state so as to compute the equilibrium lattice constants, bulk moduli and pressure derivatives as presented in Table1.

**Table 1: Lattice Constants, Bulk Moduli, Pressure Derivative, Formation and Cohesive Energy of  $\text{NiCoFeX}(\text{X}=\text{Si, As and Ge})$  in Comparison with the Work of Bahnes in the Journal of Alloys and Compounds (2017)(\*\*\*)**

Alloy	Lattice Constants( $\text{\AA}$ )	Bulk modulus(Gpa)	Pressure Derivative ( $B'$ )	Formation Energy $E_f$ ( $R_y$ )	Cohesive Energy ( $E_{coh}$ ) ( $R_y$ )
$\text{NiCoFeSi}$	6.21	5.25	6.22	-1.6864	1.6864
$\text{NiCoFeAs}$	6.31	5.33	6.23	-1.7391	1.7391
$\text{NiCoFeGe}$	6.54	5.63	6.71	-1.8439	1.8439
$\text{CoFeCrP} ***$	6.59 ***	5.32 ***	6.67 ***	-1.8543 ***	1.8543 ***
$\text{CoFeCrAs} ***$	6.74 ***	5.21***	6.54 ***	-1.7534 ***	1.7534 ***
$\text{CoFeCrSb} ***$	6.94 ***	5.61***	6.52 ***	-1.7922 ***	1.7922 ***

The quaternary heuslers (XX'YZ) has a crystallographic structure of L<sub>2</sub> type under space *Fm*3*m* (No. 225), and its structure contains four sub-lattices in which the X atoms are placed at the  $4c(\frac{1}{4}, \frac{1}{4}, \frac{1}{4})a_0$ , and  $4d(\frac{3}{4}, \frac{3}{4}, \frac{3}{4})a_0$ , and the Y and Z atoms are localized at the  $4b(\frac{1}{2}, \frac{1}{2}, \frac{1}{2})a_0$ , and  $4a(0,0,0)a_0$ , where  $a_0$  is the lattice parameter of cell (Alijani *et al.*, 2011). The calculated lattice constants, Bulk moduli and pressure derivatives of NiCoFeSi, NiCoFeAs and NiCoFeGe are shown in Table 1 as (6.21 Å, 6.31, 6.54), (5.25 Å, 5.33, 5.63) and (6.22, 6.23, 6.71) respectively. The energy of formation and cohesive energy of NiCoFeX(X=Si, As and Ge) are also investigated to ascertain whether the quaternary heuslers are structurally and synthesizable in the laboratory. If the result of the formation energy is negative and that of cohesive energy is positive, the material is structurally stable and can be synthesized experimentally and vice versa. This is done by using equitation 1 and 2:

$$E_{\text{formation}} = \text{Total Energy} -$$

$$(1) \quad (E_{\text{f}} = E_{\text{NiCoFeSi}}^{\text{Total}} - \{E_{\text{Ni}}^{\text{Bulk}} + E_{\text{Co}}^{\text{Bulk}} + E_{\text{Fe}}^{\text{Bulk}} + E_{\text{Si}}^{\text{Bulk}}\})$$

$$(2) \quad E_{\text{coh}} = \{(E_{\text{Ni}}^{\text{Total}} + E_{\text{Co}}^{\text{Total}} + E_{\text{Fe}}^{\text{Total}} + E_{\text{Si}}^{\text{Total}}) - E_{\text{NiCoFeSi}}^{\text{Total}}\}$$

Where  $E_f$  and  $E_{\text{coh}}$  represent the total formation and cohesive energies of NiCoFeSi per formula unit

respectively while  $E_{\text{Ni}}^{\text{Bulk}}$ ,  $E_{\text{Co}}^{\text{Bulk}}$ ,  $E_{\text{Fe}}^{\text{Bulk}}$  and  $E_{\text{Si}}^{\text{Bulk}}$  are the total ground state cohesive and formation energies per atom in the bulk of Ni, Co, Fe and Si as individual element of the alloy respectively (Babalola and Iyorzor, 2019). The results of formation energy show negative values while those of cohesive energy are positive, indicating that the quaternary heuslers NiCoFeX(X=Si, As and Ge) have structural stability and hence can be synthesized experimentally. In the result, it is keenly observed that the formation of energy of NiCoFeGe shows more negative values than those of NiCoFeSi and NiCoFeAs. The cohesive energy of NiCoFeGe also shows more positive value. This therefore affirms that NiCoFeGe is more structurally stable than its other two counterparts. The results of lattice constants, Bulk moduli, pressure derivatives, energies of formation and cohesive energy of NiCoFeX(X=Si, As and Ge) show good agreement with the work of A. Bahnes in the journal of Alloys and Compounds (Atifi *et al.*, 2016). In the Zinc blende structure geometry at the level of PBE-GGA, the obtained total energies data versus the cell volume of NiCoFeX(X=Si, As and Ge) are fitted by employing empirical Birch-Murnaghan Equation of states to compute the structural properties:

$$E_{\text{TOT}}(V) = E_0(V) + \frac{B_0 V}{B'(B'-1)} [B_0 \left(1 - \frac{V_0}{V}\right) + \left(\frac{V_0}{V}\right)^{B'} ] \quad (4)$$

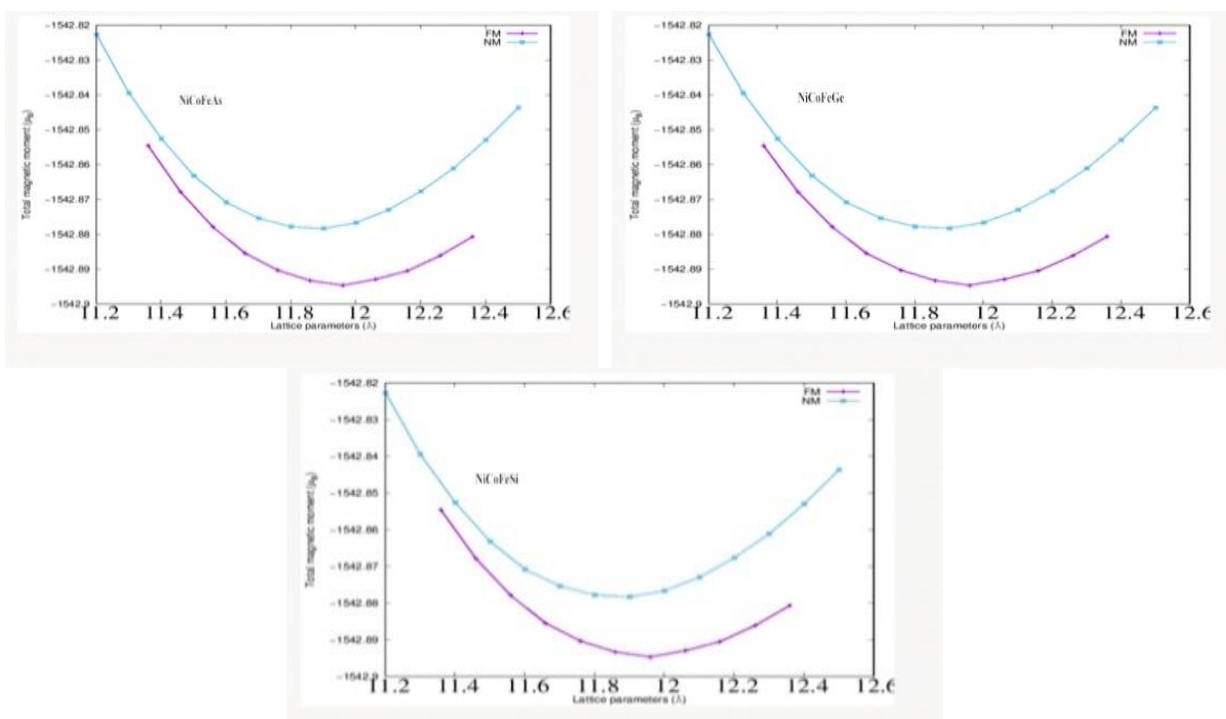


Figure 1: Graphs of Energy lattice constants of NiCoFeX(X=Si, As and Ge) in ferromagnetic and non-magnetic states

### Electronic, Half-Metallic and Magnetic Properties

They are calculated on the basis of structural and PBE-GGA parameters as presented along the high-symmetry direction in the first Brillouin zone (BZ). The majority spin states (spin-up) of the quaternary heuslers NiCoFeX(X=Si, As and Ge) exhibit semi-conducting behaviour while the minority spin states (spin-down) of the heuslers display metallic character (Bloch *et al.*, 2018). The respective indirect band gaps of NiCoFeX(X=Si, As and Ge) are 2.03eV, 1.91eV and 1.62eV respectively. The conduction band minima occur at the G-symmetry points while the valence band maxima occur at L-symmetry points in the band structures of all the alloys with respect to fermi energy level. The computed spin-polarized partial densities of states of NiCoFeX(X=Si, As and Ge) are also displayed in Fig. 3 (Atifi *et al.*, 2016). The orbital contributions of valence electrons of each element in the quaternary Heuslers cause the spin-polarization along the fermi energy level. Also, bonding and anti-bonding effects cause band gaps between the conduction band minima and valence band maxima. The valence electrons of Ni, Co, Fe, Si, As and

Ge are given as  $(3d^8, 4s^2)$ ,  $(3d^7, 4s^2)$ ,  $(3d^6, 4s^2)$ ,  $(3s^2, 3p^2)$ ,  $(3d^{10}, 4s^2, 4p^3)$  and  $(3d^{10}, 4s^2, 4p^2)$ . D-d orbital interactions within elements enhance spin-polarization of the heuslers along the fermi level (Alijani *et al.*, 2011). The bonding peaks of Ni, Co, Fe, Si, As and Ge atoms are located in the region below the fermi energy level while the region above the fermi  $E_F$  contains the anti-bonding peaks of the atoms. The contribution of bonding and anti-bonding effect of the atom cause the spin-polarization of the quaternary heuslers. Also, the d-orbital exchange splitting effect of the transition elements Ni, Co and Fe plays vital role in the spin-polarization of the heuslers. This testifies to the half-metallic character ferromagnetic nature and 100% spin-polarization of the quaternary heuslers along the fermi energy level as shown in Table 2. The half-metallic energy gap ( $E_{HM}$ ) of Heuslers is expressed as  $HM_{Gap} = \text{Min}(|E_F - E_{VBM}|, |E_F - E_{CBM}|)$ , where  $E_F$ ,  $E_{VBM}$  and  $E_{CBM}$  are the Fermi energy, valence band maximum (VBM) energy and conduction band minimum energy respectively (Babiker *et al.*, 2017).

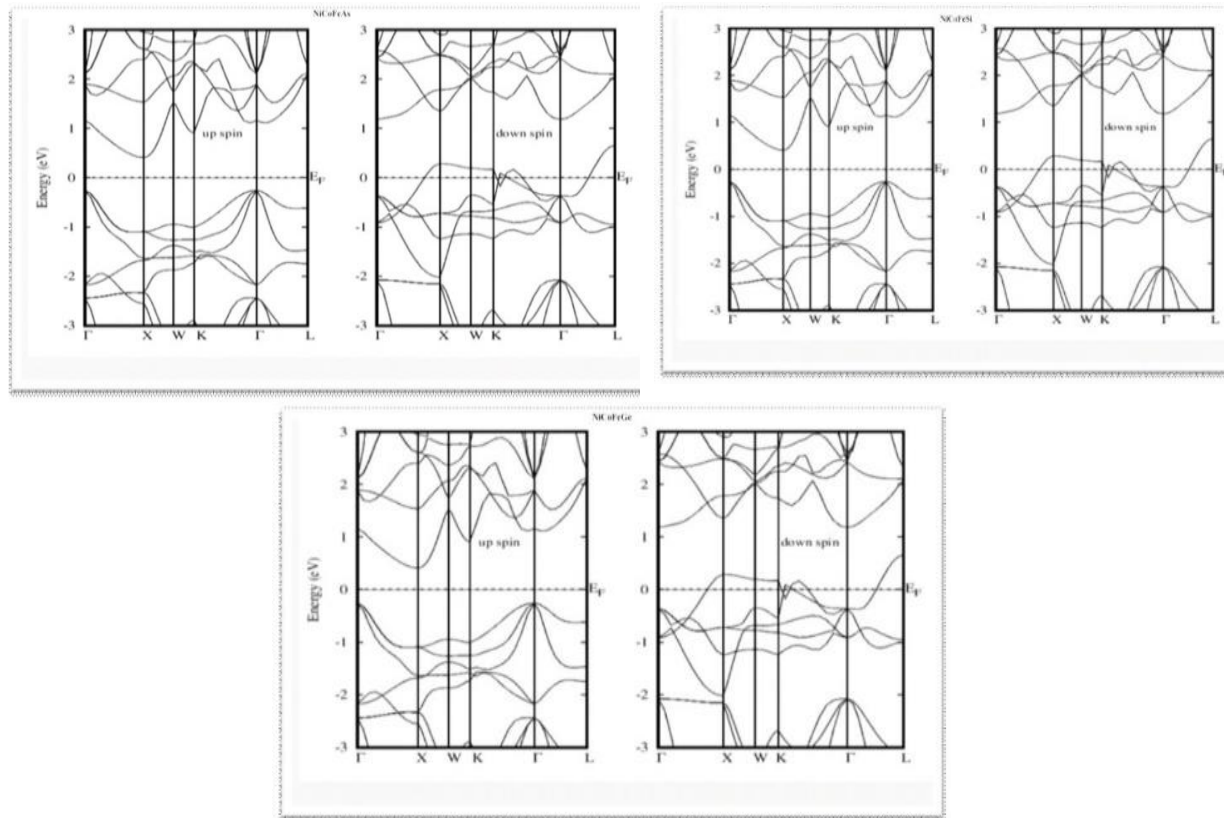


Figure 2: Spin-polarized Electronic Band structures of NiCoFeSi, NiCoFeAs and NiCoFeGe

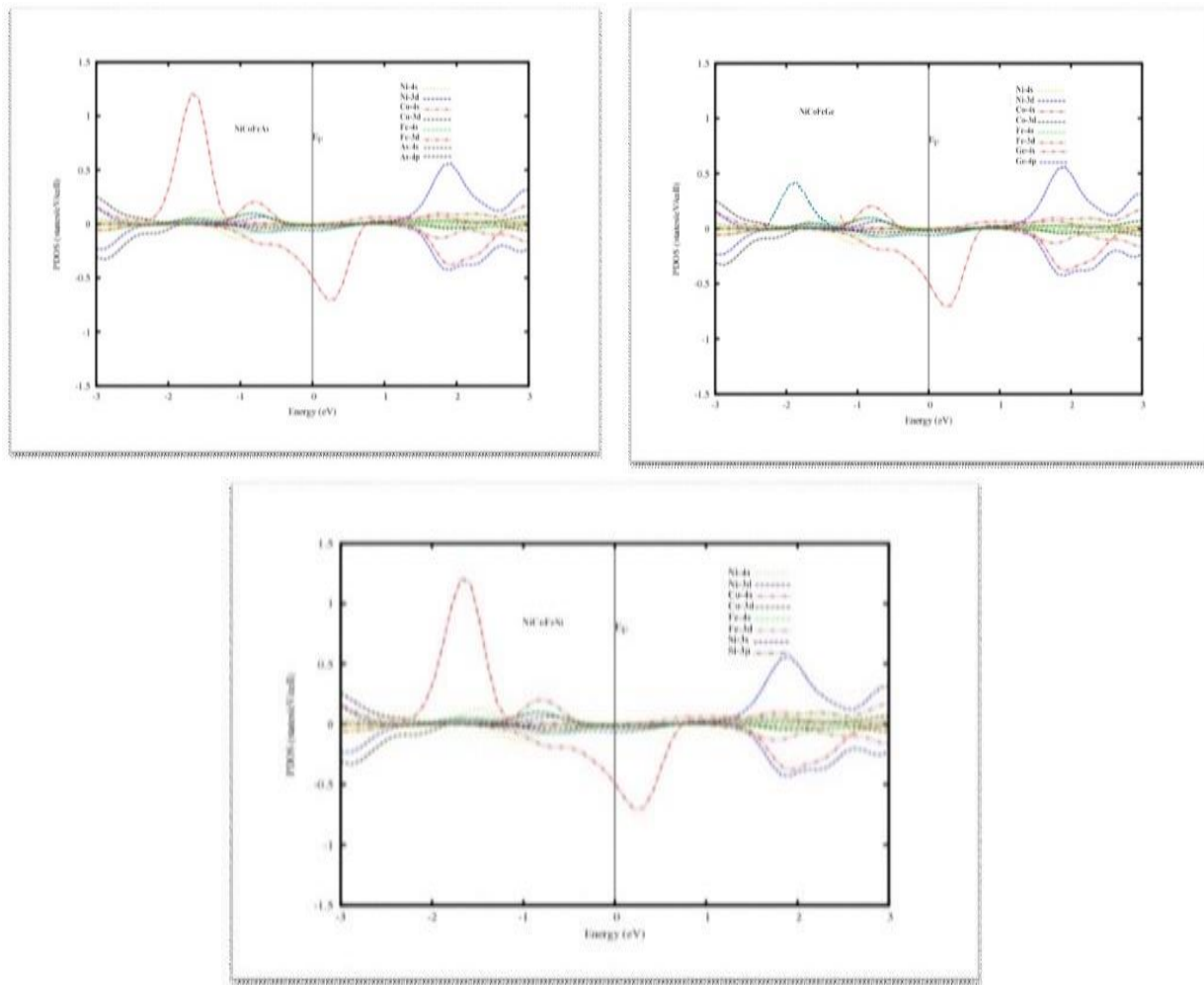


Figure 3: Spin-Polarized Partial Densities of States of NiCoFeX(X=Si, As and Ge)

**Table 2: Calculated Results of the Half-Metallic Gap  $E_{HM}$  (eV), Minority Spin ( $P \downarrow$ ), Majority Spin ( $P \uparrow$ ), Band Gap  $E_g$  (eV) and Spin Polarization Percentage at the Fermi Energy Level  $E_F$  of NiCoFeX(X=Si, As and Ge) and CoFeCrZ(Z=P,As and Sb).\*\*\***

Alloy	$E_{HM}$ (eV)	$E_g$ (eV)	$P \uparrow$ (eV)	$P \downarrow$ (eV)	$P$ (%)
<i>NiCoFeSi</i>	1.206	1.206	1.206	0.000	100
<i>NiCoFeAs</i>	1.205	1.205	1.205	0.000	100
<i>NiCoFeGe</i>	0.903	0.903	0.903	0.000	100
<i>CoFeCrP</i> ***	1.000 ***	1.000 ***	1.000 ***	0.000 ***	100 ***
<i>CoFeCrAs</i> ***	0.520 ***	0.520 ***	0.520 ***	0.000 ***	100 ***
<i>CoFeCrSb</i> ***	0.750 ***	0.750 ***	0.750 ***	0.000 ***	100 ***

The spin-polarization percentage of a half-metallic material is described by the repartition of the densities of states (DOSs) in spin-up and spin-down cases at the  $E_F$ , which it is defined by the following expression

$$P(\%) = \frac{P \uparrow(E_F) - P \downarrow(E_F)}{P \uparrow(E_F) + P \downarrow(E_F)} \times 100\% \quad (5)$$

Here,  $P \uparrow(E_F)$  and  $P \downarrow(E_F)$  are the densities of majority and minority spin electrons at  $E_F$ , respectively. The complete half-metallic character is observed when  $P \downarrow(E_F)$  or  $P \uparrow(E_F)$  is equal to zero (Babalola and

Iyorror, 2019). The partial and total magnetic moments of NiCoFeX(X=Si, As and Ge) are also computed as shown in Table 3. The total magnetic of NiCoFeX(X=Si, As and Ge) is in line with the analytical proof of the Slater Paulin's rule ( $M_T = Z_T - 24 \geq 1$  for full or quaternary heuslers as our evaluated total magnetic moments are greater than one, which thus obey Slater Paulin's rule (Bahnes *et al.*, 2017). If  $M_T$  is greater than or equal to one it shows that the material is ferromagnetic but if it is equal to zero it is non-magnetic.

**Table: 3 Total and Partial Magnetic Moments and Curie Temperature,  $T_c$  of NiCoFeX(X=Si,As and Ge) (from pdos.out file) and the Results of Bahnes in the Journal of Alloy and Compounds (2017) denoted by \*\*\***

Alloy	$M_{Ni}(\mu_B)$	$M_{Co}(\mu_B)$	$M_{Fe}(\mu_B)$	$M_X(\mu_B)$	$M_{Tot}(\mu_B)$	$T_c(K)$
<i>NiCoFeSi</i>	0.6229	1.7486	0.7598	0.8902	4.0215	526
<i>NiCoFeAs</i>	0.7831	1.6286	0.7693	0.9763	4.1573	859
<i>NiCoFeGe</i>	0.8356	1.8748	0.9842	0.9765	4.6711	2631
<i>CoFeCrP</i> ***	1.2220***	1.2630***	0.4060***	1.1111***	4.0000 ***	759 ***
<i>CoFeCrAs</i> ***	1.2300***	1.1553***	0.5050****	1.1120***	4.0000 ***	759 ***
<i>CoFeCrSb</i> ***	1.2000***	1.1830***	0.5060***	1.1110***	4.0000 ***	759 ***

### Mechanical and Thermodynamic Properties

The calculated mechanical properties of NiCoFeX(X=Si, As and Ge) such as elastic constants ( $C_{11}$ ,  $C_{12}$ ,  $C_{44}$ ), Shear modulus (G), Pugh's index ( $B/G$ ), Young's modulus, poisson's ratio (v), Cauchy Pressure ( $C_{12} - C_{44}$ ) and Zener Anisotropy factor (A) are shown in Table3. Our calculated elastic constants ( $C_{11}$ ,  $C_{12}$ ,  $C_{44}$ ) and Bulk modulus (B) are positive. This satisfies mechanical stability criteria given as  $C_{11} - C_{12} > 0$ ,  $C_{11} > 0$ ,  $C_{44} > 0$ ,  $(C_{11} + 2C_{12}) > 0$  and  $C_{12} < B < C_{11}$ , indicating that NiCoFeSi, NiCoFeAs and NiCoFeGe have greater resistance against mechanical stress and deformations (Born *et al.*,2016). For ductility of material to be achieved Pugh's index, poisson's ratio and Cauchy Pressure must be greater than 1.75, 0.26 and positive respectively. From Table3, our Pugh's index, poisson's ratio, Cauchy Pressure are 2.05,1.82 and 3.25 respectively. This indicates that the quaternary heuslers are ductile. If these calculated values are less than that the given standard values, it means the materials are brittle. For a material to be isotropic its Zener Anisotropic factor must be equal to equal to unity (i.e 1), if it is greater than unity it is anisotropic. It must have the same alignment or orientation in all sides, and there is possibility of developing micro-cracks in future. However, our calculated value of Zener Anisotropy factor is greater than one ( $A > 1$ ), indicating that the material is anisotropic. This is also shown in Table 3 (Chibani *et al.*,2018). However, for the sake of clarity equations of the mechanical properties are given here-under:

$$B_{VRH} = \frac{1}{2}(B_V + B_R), B_{VRH} = \frac{1}{2}(G_V + G_R) \quad (6)$$

$$\text{Where } B_{V,R} = \frac{1}{3}(C_{11} + 2C_{12}), G_R = \frac{5(C_{11} - C_{12})C_{44}}{4C_{44} - 3(C_{11} - C_{12})}, \\ G_V = \frac{1}{5}(C_{11} - C_{12} + 3C_{44}) \quad (7)$$

The calculated elastic constants are listed in Table 3 with selected mechanical properties such as bulk, shear and Young's moduli, and Poisson's ratio . Isotropic Crystals are those which their atomic patterns have such a high degree of symmetry that their properties do not vary in different orientations (relative to their atomic patterns)

(Fazian *et al.*,2016). Also, the Zener Anisotropy factor can be calculated by

$$A = \frac{2C_{44}}{C_{11} - C_{12}} \quad (8)$$

The value of A=1 gives purely isotropic system and the deviation from this value measures by percentage of Anisotropy,  $A_G$ .

$$A_G = \frac{G_V - G_R}{G_V(G_V + G_R)} \quad (9)$$

If an alloy or compound has A greater than unity it shows that there is elastic anisotropy. Then, there will be possibility of developing more micro -cracks or structural defects during the growth process of the alloy or compound. Cauchy Pressure (CP) is also calculated in this work. It is shown by Petit that CP is given by

$$CP = C_{12} - C_{44} \quad (10)$$

Cauchy Pressure determines brittle or ductile nature of materials. CP value is a measure of metallic bonding or directional bonding with the angular character. If its value is positive, it indicates ductility and vice versa. Pugh's ratio B/G proposed by Pugh also measures ductility and brittleness (Atifi *et al.*,2016). A material is said to have ductile behaviour if  $B/G \approx 1.75$ . Any B/G value less than 1.75 shows brittleness of the material.

The Poisson's ratio V is another parameter for measuring ductility and brittleness.

$$V = \frac{(3B - 2G)}{2(3B + G)} \quad (11)$$

If the value of  $V \approx 0.26$ , then the material is ductile and vice versa. The ratio of linear stress to strain is called Young's Modulus Y. Its higher value for a material means higher stiffness. With the increase in E, there is also increase in the covalent property of the material which has then impacted on the ductility of a material (Andrea *et al.*,2008) . Young's modulus is defined in terms of bulk and shear moduli B and G as follows:

$$Y = \frac{9BG}{3G + B} \quad (12)$$

The higher value of E indicates stiffness of the material. Generally, the shear modulus G indicates the resistance to plastic deformation while Bulk modulus B stands for resistance to fracture (Babalola and Iyozor,2019).

**Table 4: Calculated Elastic Constants ( $C_{ij}$ ) (Gpa), Bulk Modulus ( $B$ ) (Gpa), Shear Modulus ( $G$ ) (Gpa), Young's Modulus ( $Y$ ) (Gpa), Poisson's Ratio ( $\nu$ ), Anisotropy Factor ( $A$ ), Pugh's Ratio ( $B/G$ ) and Cauchy's Pressure ( $C_{12} - C_{44}$ ) of NiCoFeSi, NiCoFeAs and NiCoFeGe and the Results of CoFeCrZ (Z=P, As and Sb) \*\* by Bahnes (2017).**

Heusler Alloy	$C_{11}$	$C_{12}$	$C_{44}$	$B$	$G$	$Y$	$\nu$	$A$	$B/G$	$C_{12} - C_{44}$
NiCoFeSi	347	231	205	242	121	235	0.29	3.56	2.00	26
NiCoFeAs	352	234	206	248	123	238	0.29	3.80	2.01	38
NiCoFeGe	364	244	209	251	128	246	0.28	16.80	2.00	115
CoFeCrP**	265**	161**	128**	234**	89**	237**	0.33**	2.40**	2.63**	33**
CoFeCrAs**	240**	190**	119**	209**	64**	174**	0.36**	4.82**	3.26**	71**
CoFeCrSb**	218**	168**	168**	185**	65**	174**	0.34**	4.74**	2.85**	48**

For thermodynamic properties of NiCoFeX (X=Si, As and Ge), the heat capacity ( $C_V$ ) Versus temperature graphs are plotted in fig.4. This is in accordance with the thermodynamic equations below.

For classical thermodynamic process,

$$\langle n_s \rangle = \frac{1}{\frac{\hbar\omega}{e^{KT}-1}} \quad (13)$$

The internal energy of the alloy is

$$E = \int_0^{\omega_D} \hbar\omega \langle n_s \rangle \sigma(\omega) d\omega \quad (14)$$

$$E = \int_0^{\omega_D} \hbar\omega \frac{1}{e^{KT}-1} \cdot \frac{9N}{\omega_D^3} \omega^2 d\omega \quad (15)$$

$$\text{Putting } x = \frac{\hbar\omega_D}{KT}, E = \frac{9Nh}{\omega_D^3} \left(\frac{KT}{\hbar}\right)^4 \int_0^{\hbar\omega_D} \frac{x^3}{e^x - 1} dx,$$

$$\text{Let } \theta_D = \frac{\hbar\omega_D}{K}. \quad (16)$$

Then,  $\theta_D$  is the Debye characteristic Temperature,

$$E = \frac{9Nh}{\omega_D^3} \left(\frac{KT}{\hbar}\right)^4 \int_0^{\theta_D} \frac{x^3}{e^x - 1} dx \quad (17)$$

If  $T >> \theta_D$ ,  $x_{max} = \frac{\hbar\omega_D}{KT} = \frac{\theta_D}{T}$  is small and, expanding the exponential and neglecting the higher powers;

$$\frac{e^x}{e^x - 1} = x^2$$

Therefore,

$$E = \frac{9NKT^4}{\theta_D^3} \left[ \frac{x^3}{3} \right]_{\theta_D/T} = \frac{9NKT^4}{\theta_D^3} \cdot \frac{\theta_D^3}{3T^3}, E = 3NKT \quad (18)$$

This leads to the Dulong - Petit law

$$C_V = \left( \frac{\partial E}{\partial T} \right)_V = 3NK = 3R \quad (19)$$

Where  $R = KN$  is the molar gas constant.

Thus, for temperature greater than the Debye Temperature, the alloy behaves classically.

If on the other hand,  $T << \theta_D$ ,  $x \rightarrow \infty$ , then,

$$\int_0^{\infty} \frac{x^3 dx}{e^x - 1} = \int_0^{\infty} \frac{x^3 dx}{e^x(1-e^{-x})} = \int_0^{\infty} x^3 e^{-x} (1 - e^{-x})^{-1} dx \quad (20)$$

$$= \int_0^{\infty} x^3 e^{-x} (1 - e^{-x} + e^{-2x} + e^{-3x} + \dots) dx \quad (21)$$

$$= \int_0^{\infty} x^3 \sum_{n=1}^{\infty} e^{-nx} dx \quad (22)$$

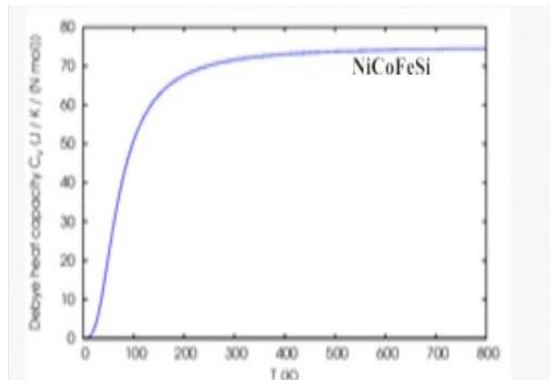
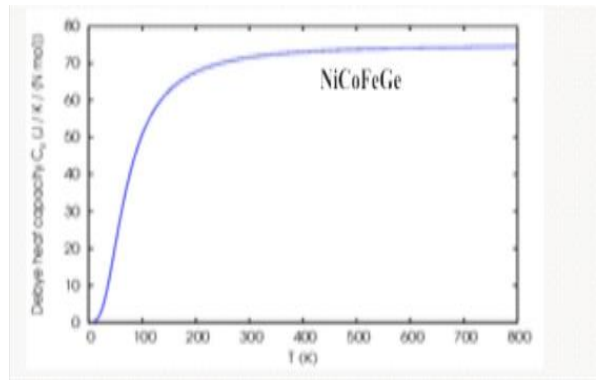
$$\text{Using gamma function : } \int_0^{\infty} x^3 \sum_{n=1}^{\infty} e^{-nx} dx = \sum_{n=1}^{\infty} \frac{3!}{n^4} = 3! \sum_{n=1}^{\infty} \frac{1}{n^4},$$

$$\text{Using complex variables, } \int_0^{\infty} \frac{x^3 dx}{e^x - 1} = \frac{\pi^4}{15} \quad (23)$$

$$\text{Thus, } E = \frac{9NKT^4}{\theta_D^3} \cdot \frac{\pi^4}{15} = \frac{3\pi^4 NKT^4}{5\theta_D^3}, \text{ and the specific heat}$$

$$C_V = \left( \frac{\partial E}{\partial T} \right)_V = \frac{3\pi^4 NK \partial T^4}{5\theta_D^3 \partial T} = \frac{3\pi^4 NK 4T^3}{5\theta_D^3} \quad (23)$$

$$C_V = \frac{12}{5} \pi^4 NK \left( \frac{T}{\theta_D} \right)^3 \quad (24)$$



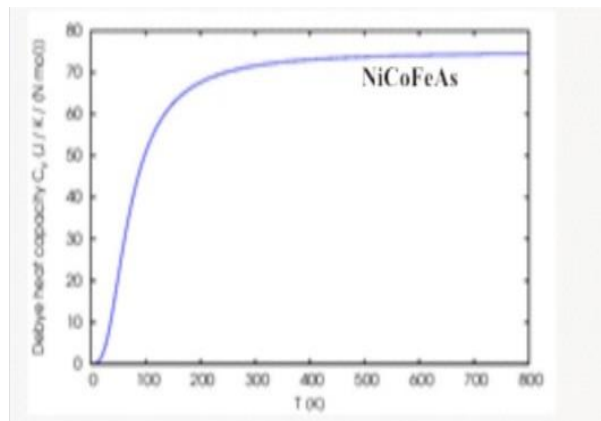


Figure.4: Heat Capacities Versus Temperatures of of NiCoFeX(X=Si, As and Ge)

The constant-volume heat capacity  $C_V$ , tends to the Dulong-Petit limit at high temperature (i.e it remains constant) but at sufficiently low temperature, the heat capacity of NiCoFeSi, NiCoFeAs and NiCoFeGe is proportional to  $T^3$  (Babiker *et al.*,2017). This is verified analytically in eqs.(5-15). It is observed that from 256K above, the constant-volume heat capacity for each heusler alloy approaches asymptotic value of 75J/mol and obeys Dulong-Petit law which states that at high temperature heat capacity of material remains constant but at sufficiently low temperature (0k) the heat capacity of material is proportional to  $T^3$ ,showing that it obeys  $T^3$  law at sufficiently low temperature and obeys Dulong-Petit law at high temperature.This remarkable thermodynamic behaviour has good applications in the field of solid states physics where half-metallicity, ferromagnetism or 100% spin-polarization is of great importance in spintronic, optoelectronics etc.

## CONCLUSION

First Principles calculations have been used to study the half-metallic behaviour, structural, mechanical, magnetic, electronic and thermodynamic properties of quaternary heuslers NiCoFeX(X=Si, As and Ge). The results of the structural properties show that the heusler alloys are structurally stable and can be synthesized experimentally. All mechanical properties of the quaternary heuslers obey mechanical stability criteria as they show high ductility and greater resistance against deformations. The electronic band structures of NiCoFeX(X=Si, As and Ge) give indirect band gaps which justifies their half-metallic character and 100% spin-polarization at the fermi energy levels. The total magnetic moments of the heusler alloys obey Slater-Paulin's rule, which indicates that the materials are ferromagnetic. Thermodynamic heat capacities of NiCoFeX(X=Si, As and Ge) show good thermal behaviour as it obeys  $T^3$  law at sufficiently low temperature and also obeys Dulong-Petit law at high temperature. This portrays great potentials of the

quaternary heuslers in the field of spintronic, optoelectronics etc. Our results are in good agreement with the results in literatures.

## REFERENCES

Akriche, A.; Bouafia, H.; Hiadsi, S.; Abidri, B.; Sahli, B.; Elchikh, M.; Djebour, B.(2017) First-principles study of mechanical, exchange interactions and the robustness in  $\text{Co}_2\text{MnSi}$  full Heusler compounds. *J. Magn. Magn. Mater.* 422, pg.13–19.

Alijani, V.; Ouardi, S.; Fecher, G.H.; Winterlik, J.; Naghavi, S.S.; Kozina, X.; Ueda, S.(2011) Electronic, structural, and magnetic properties of the half-metallic ferromagnetic quaternary Heusler compounds  $\text{CoFeMnZ}$  ( $Z = \text{Al, Ga, Si, Ge}$ ). *Phys. Rev. B.* 84, pg.22-44.

Andrea M., Conor H., Myrta G.(2008) Yambo ab initio calculation tool for excited state calculations. 50, pg.1-20.

Atifi Sattar M., Muhammad Rashid, Raza Hashmi, Fayyat Hussain .(2016) study of half-matalicity Journal of Chinnese Physical Society and IOP .Vol.25,No.10. pp10702-7

Babalola M.I, Iyozor B.E : (2019) A search for half-metallicity in half-Heusler alloys,  $\text{HfFeBi}$  and  $\text{TiFeBi}$  . *Journal of magnetism and magnetic materials.*,165560, pp491-506.

Babiker, S.; Gao, G.; Yao, K. Half-metallicity and magnetism of Heusler alloys  $\text{CO}_2\text{HfZ}$  ( $Z = \text{Al, Ga, Ge, Sn}$ ).(2017) *J. Magn. Magn. Mater.* 441, pg.356–360.

Bahnes A., Boukortt A., Abbassa H., Almough D.E, Hyan A. Zaoul. Half-metallic ferromagnetic behaviour of a new quaternary Heusler compounds  $\text{CoFeCrZ}$  ( $Z = \text{P, As, and Sb}$ ).(2017) *Journal. of Alloys and Compounds.* 424, pg.22–77.

Bainsla, L.; Mallick, A.I.; Coelho, A.A.; Nigam, A.K.; Varaprasad, B.C.S.; Takahashi, Y.K.; Hono, K.(2015) High spin polarization and spin splitting in equiatomic quaternary CoFeCrAl Heusler alloy. *J. Magn. Magn. Mater.* 394, pg.82–86.

Bainsla, L.; Mallick, A.I.; Raja, M.M.; Nigam, A.K.; Varaprasad, B.C.S.; Takahashi, Y.K.; Hono, K. (2015) Spin gapless semiconducting behavior in equiatomic quaternary CoFeMnSi Heusler alloy. *Phys. Rev. B*, 91, pg.104-408.

Bainsla, L.; Suresh, K.G., Artimeb B.V . Equiatomic quaternary Heusler alloys: A material perspective for spintronic applications. *Appl. Phys. Rev.* (2016), 031101 pg.32-45.

Blöch, P.E., Avengular B.N, Chenvzenco F.K . Projector augmented-wave method. (2018) (Phys. Rev. B 50, pg.17-53.

Born, M., Huang K.L, Hoboken N.J, John W.(2016) Dynamical Theory of crystal Lattices. “Born-Oppenheimer Approach : Diabatization and Topological Matrix” Beyond Born-Oppenheimer : Electronic

Nonadiabatic coupling Terms and conical Intersection. *Journal of phy. Rev.*, 2246, pg. 26-57.

Chibani, S.; Arbouche, O.; Zemouli, M.; Amara, K.; Benallou, Y.; Azzaz, Y.; Ameri, M.(2018) Ab Initio Prediction of the Structural, Electronic, Elastic, and Thermoelectric Properties of Half-Heusler Ternary Compounds TiIrX (X = As and Sb). *J. Electron. Journal of Mater. Sc.* 47, pg.196–204.

De Groot, R.A.; Mueller, F.M.; Van Engen, P.G.; Buschow, K.H.J.(1983) New class of materials: Half-metallic ferromagnets. *Phys. Rev. Lett.* 50, pg.20-24.

Fazian M., Murtaza G., Sikandar A., Saleem A.K, Asif M.,(2016) Elastic and Optoelectronic properties of novel  $Ag_3AuSe_2$  and  $Ag_3AuTe_2$  semiconductors . *Journal of material science in semiconductor processing.* 4537, pg.8–15.

Feng, Y.; Chen, X.; Zhou, T.; Yuan, H.; Chen, H.(2015) Structural stability, half-metallicity and magnetism of the CoFeMnSi/GaAs interface. *Appl. Surf. Sci.* 346,pg.1–10.

Feng, Y.; Xu, X.; Cao, W.; Zhou, T.(2018) Investigation of cobalt and silicon co-doping in quaternary Heusler alloy NiFeMnSn. *Comput. Mater. Sci.* 147,pg. 251–257.